Journal of Analytical and Applied Pyrolysis 116 (2015) 263–271

Contents lists available at ScienceDirect

Journal of Analytical and Applied Pyrolysis

journal homepage: www.elsevier.com/locate/jaap

Chemical structure evolution of char during the pyrolysis of cellulose

Shanzhi Xin[a,b], Haiping Yang[a,*], Yingquan Chen[a], Mingfa Yang[a], Lei Chen[a], Xianhua Wang[a], Hanping Chen[a]

[a] State Key Laboratory of Coal Combustion, Huazhong University of Science and Technology, Wuhan 430074, China
[b] Hubei Key Laboratory of Industrial Fume & Dust Pollution Control, Jianghan University, Wuhan 430056, China

ARTICLE INFO

Article history:
Received 24 April 2015
Received in revised form 1 September 2015
Accepted 2 September 2015
Available online 8 September 2015

Keywords:
Cellulose
Pyrolysis
Char
Intra-/intermolecular H-bonds
Aromatic structure

ABSTRACT

The formation and evolution of chemical structure of char during cellulose (ash-free) pyrolysis were investigated using two-dimensional infrared correlation spectroscopy combined with Raman spectroscopy. The initial temperature at which water evolved chemically from cellulose pyrolysis is around 200 °C. The cleavage of intra- and inter-molecular hydrogen bonds (H-bonds) and the subsequent dehydration were the primary reactions as temperature below 300 °C, among which intra-molecular dehydration was the predominated reaction. However, dehydration occurred principally inter-molecularly along with decarbonylation, ring-opening and aromatization at temperature over 300 °C. The concentration of carbonyl, conjugated olefin, ether and aromatic structure increased significantly at the expense of glycosidic bond, pyran ring and hydroxyl groups diminishing in the residual char. The oligosaccharides, aliphatic hydrocarbons and aromatics were bonded through the ether linkage to form a disordered three-dimensional network. Dehydration was almost accomplished at 430 °C and smallest aromatic clusters grafted with oxygenated groups underwent significant deoxygenation and condensation at 430–650 °C. The predominant reaction shifted from deoxygenation toward dehydrogenation as the temperature exceeded 650 °C and the char was highly aromatic with large aromatic systems composed of over six fused ring structures. The study provides insightful details into the initial stage of cellulose degradation.

1. Introduction

Biomass is the only carbon-containing renewable source that can be used for producing a variety of gas, liquid and solid fuels or chemicals via pyrolysis [1]. Cellulose is the most abundant natural polymer on earth and the largest fractions in lignocellulosic biomass (approximately 50% by weight) [2]. Cellulose is a linear homopolymer of β-1,4-1inked D-glucopyranose units and the cellulose microfibrils constitute the skeleton of cell walls which is embedded in a matrix composed of hemicellulose, lignin, and other carbohydrate polymers [3]. The abundant hydroxyl groups in cellulose macromolecular give rise to networks of strong hydrogen bonding. In general, each glucose unit contains the same hydrogen bonding network with two intra-molecular bonds and one inter-molecular bond [4,5].

A number of studies have been carried out to investigate the thermal degradation of cellulose [6–13]. It was found that the pyrolysis of cellulose was characterized by a high yield of liquid and low yield of char [6]. Therefore, the properties of released products, such as gases and liquids, had aroused widespread attentions [11–13]. Nevertheless, the formation and evolution of char structure are critical to describe the pyrolysis chemistry and total product distribution [14–17]. For example, additional heating can lead to the release of volatiles from the char. Meanwhile, the surface and structure properties of char can affect the reactivity of char and its combustion behaviors [14,15]. Therefore, the elucidation of the char formation of cellulose, especially the initial stage of pyrolysis and the aromatic structure evolution at high temperature is particularly beneficial for achieving a better understanding of the pyrolytic behavior of biomass.

One of the earliest proposed mechanism of cellulose degradation is the "Broido-Shafizadeh model" [18]. In this model, the initiation process is the conversion of cellulose to "active cellulose" intermediate and the followed by two competing pathways to produce char and volatile species. However, although the concept of "active cellulose" was proposed for many years, no detailed description of the nature of active cellulose has been developed [19]. Therefore, some studies assume that no such intermediate

* Corresponding author. Fax: +86 27 87545526.
E-mail address: yhping2002@163.com (H. Yang).

http://dx.doi.org/10.1016/j.jaap.2015.09.002
0165-2370/

exists during cellulose pyrolysis, probably because the difficulties in the identification of intermediate products.

To date, most of the studies focused on the char formation at temperatures which cellulose underwent apparent depolymerization. Tang and Bacon [20] pyrolyzed cellulose up to 500 °C and the carbonization process was classified into four successive stages: desorption of adsorbed water, splitting off the structure water, chain scissions and aromatization. Shafizadeh and Sekiguchi [21] observed a rapid weight loss and development of aromatic structures between 350 and 400 °C. As temperature increased further, the amount of aromatic carbon remained constant. However, Sekiguchi et al. [22] suggested that the aromaticity of the char was further increased at 400–500 °C. The pyrolysis of cellulose was conducted by Boon et al. [23] and Pastorova et al. [24] using combined approaches, such as PY-MS, PY-GC/MS, FTIR, NMR and wet chemical techniques. They found that, at 250 °C, cellulose lost linearity to form a three-dimensional network polymer, which is rich in carboxyl and carbonyl groups and had the furanoid and hydroxyaromatic skeletons. Wooten et al. [14] identified a carbohydrate intermediate "final carbohydrate" from cellulose pyrolysis and the intermediates were preferentially converted to aromatics rather than aliphatic groups.

Fourier transform infrared spectroscopy (FTIR) technology was frequently used to study the surface chemistry of chars [25,26]. However, remarkable peak overlaps of the conventional infrared spectra make it difficult to describe the changes in specific bonds. The two-dimensional (2D) infrared correlation spectroscopy developed by Noda is a powerful tool that can be used to evaluate the differences of spectra observed during an external perturbation [27,28]. This method enhances the resolution of spectra obtained by traditional ways and provides important information about the surface functionality of solid residual which cannot be revealed through conventional infrared and its derivative spectra [26]. Although this method was applied in studying polymeric materials widely, few studies have been done on the biochar formation process. Harvey et al. investigated the biochar formation process of different biomass samples under oxygen limited conditions [29]. However, the structural evolution of cellulose is different from that of lignocelluloses biomasses.

Watanabe et al. [30] investigated the structural changes in hydrogen bonds in cellulose by infrared (IR) and near-infrared (NIR) based moving-window 2D correlation spectra. It was found that the strong H-bonds in cellulose occurred structural changes in the range of 25–130 °C and resulted in the formation of very weak H-bonds in 40–90 °C. The scission of H-bonds in I_α phase occurs mainly at 40–100 °C and it is completed below 180 °C. Regarding I_β phase in cellulose, the band intensities of O3—H3···O5 and O2—H2···O6 intrachain H-bonds showed a remarkable decrease at 220 °C, whereas that of interchain H-bonds are not observed adequately[31]. Agarwal et al. modeled the structural transformation of cellulose I_β to a high temperature (550 K) and found that I_β phase is dominated by intrachain H-bonds at 300–400 K and weaker interchain H-bonds at 450–550 K [32]. Therefore, it can be seen that the change of H-bonds certainly exists in the initial stage of cellulose pyrolysis and shows a strong correlation with the structural change. Nevertheless, to the best of our knowledge, the pyrolysis chemistry of such a process was rarely discussed in the literature. However, the identification of inter- and intra-molecular H-bond in cellulose and the change of the H-bond during the initial stage of pyrolysis is important for the understanding of the whole pyrolytic behavior for cellulose [33].

Furthermore, the structure evolution of biochar at higher temperatures, such as the changes in degree of graphitization and size of aromatic clusters, is also important for understanding the overall degradation mechanism of cellulose. Therefore, in this study, the char formation during the low temperature pyrolysis of cellulose was investigated by two-dimensional infrared correlation spectroscopy. Furthermore, we combined this method with the Raman and other approaches to investigate the structure evolution of char at a higher temperature. The objective was to provide a detailed description of the char structure evolution and cellulose degradation of cellulose at a wider temperature range (200–950 °C).

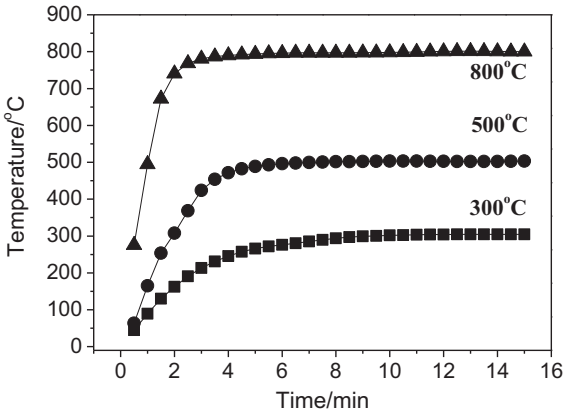

Fig. 1. Temperature-time profile of cellulose sample at 300 °C, 500 °C and 800 °C.

2. Material and methods

2.1. Cellulose sample

The cellulose sample was provided by Sigma–Aldrich Co., Ltd. It was in the form of white and microcrystalline powders of 20 μm particle size. The cellulose contained 42.7 wt.% of C, 6.2 wt.% of H, 51 wt.% of O and trace amount of N and S on a dry ash free basis. No ash has been detected according to ASTM method (D1102-84). Proximate analysis was performed on dry basis and the result indicated that the volatile matter of cellulose was as high as 95.5 wt.% and the amount of remaining fixed carbon was only 4.5 wt.%. The low heat value of cellulose (contained 5% of moisture) was 15.47 MJ/kg.

2.2. Preparation of cellulose chars

The pyrolysis char was obtained in a bench-scale fixed bed reactor at temperatures ranging from 200 to 950 °C under nitrogen (99.999%, 200 mL/min) for 30 min, following the procedures described in our previous study [6]. Prior to each trial, the reactor was heated up to the designated temperature with nitrogen as carrier gas and kept constant for 10 min in order to exchange the air in the quartz tube. After that, a porcelain crucible loaded with a thin layer of cellulose was quickly pushed into the center of the reactor. Cellulose sample occurred pyrolysis when the porcelain crucible reached the center of heating furnace. Then, the crucible was moved to the sweep gas inlet when the pyrolysis was finished and cooled down with nitrogen (1 L/min) to ambient temperature instantly. The amount of char fractions was determined based on the weight differences of the porcelain crucible. The experimental error in the yield measurements was less than ±1.0%.

During the pyrolysis experiment, the temperature-time profile of cellulose sample was measured by inserting a thermocouple in the sample bed. Fig. 1 shows the temperature measured as a function of time for final pyrolysis temperature of 300 °C, 500 °C and 800 °C. It can be seen that, in the initial stage of pyrolysis, the heating rate of cellulose sample was in the range of about 30–300 °C/min.

2.3. Characterization of char

The elemental composition of the resulting char was determined using a CHNS/O elementary analyzer (Vario Micro cube, Germany). The contents of carbon, hydrogen, nitrogen were determined directly, while the oxygen content was calculated by difference. The element composition of char is presented in the form of Van Krevelan diagram, which plotted H/C atomic ratio against the O/C to characterize the degree of aromaticity and maturity.

Surface functionality of char was analyzed quantitatively with FTIR spectroscopy (VERTEX 70 Bruker, Germany). The spectra were recorded in the range of 400–4000 cm^{-1} and each spectrum was the result of 120 accumulated scans with 4 cm^{-1} resolution. The testing procedure was described elsewhere in detail [16]. Each spectrum was subjected to smoothing (Savitizy–Golay method) and baseline correction in the analysis windows. After that, the spectrum was transformed into Kubelka–Munk unit. All the data treatment procedures were performed using the Omnic software (Version 8.0, Thermo-Fisher Scientific) introduced by Harvey et al. [29].

The two-dimensional (2D) correlation spectroscopy was calculated using the generalized 2D correlation method developed by Noda and Ozaki [27]. The intensity of 2D correlation spectrum $X(\nu_1, \nu_2)$ represents the quantitative similarity or dissimilarity between changes in the intensity of two different spectral variables (ν_1 and ν_2) along the external variable t during a fixed interval (T_{min} to T_{max}). The 2D correlation spectrum can be expressed as:

$$X(\nu_1, \nu_2) = \langle \tilde{y}(\nu_1, t) \times \tilde{y}(\nu_2, t) \rangle \quad (1)$$

The symbol $\langle\rangle$ denotes a cross-correlation function designed to compare the dependence patterns of two chosen quantities on t. In order to simplify the mathematical manipulation, $X(\nu_1, \nu_2)$ is treated as a complex number function:

$$X(\nu_1, \nu_2) = \Phi(\nu_1, \nu_2) + i\Psi(\nu_1, \nu_2) \quad (2)$$

The intensity of a synchronous 2D correlation spectrum $\Phi(\nu_1,\nu_2)$ represents the simultaneous or coincidental changes of two separate spectral variations measured at ν_1 and ν_2. Correlation peaks appear at both diagonal and off-diagonal positions. The auto peaks located at the diagonal position ($\nu_1 = \nu_2$) exclusively appear in the synchronous 2D spectra and represent vibrations that are most susceptible to changes in the external perturbant. Any region of a spectrum which changes intensity to a great extent will show strong autopeaks. On the other hand, cross peaks $\Psi(\nu_1,\nu_2)$ at the off-diagonal positions can be found in both synchronous and asynchronous spectra and can be either positive or negative. Combination of synchronous and asynchronous spectra provides the general direction and the sequence of change in different groups. The detailed information regarding the fundamental concept and their interpretation can be found elsewhere [27,28]. The Noda's rules for interpreting the cross peaks were summarized by Harvey et al. as shown in Table S1 [29]. This method was adopted by Chen et al. in our group to study the evolution of functional groups during cotton and corn stalks torrefaction [34].

The Fourier transform-Raman (FT-Raman) spectra of resultant char were recorded using Bruker's VERTEX-70 Series spectrometer following the procedures described by Li et al. [35]. The light source for Raman spectroscopy was a Nd: YAG laser at 1064 nm, and the spectra were collected using an InGaAs detector at room temperature. Laser power was 250 mW, and every spectrum represented the average of 80 scans. The Raman spectra in the range of 1800–800 cm^{-1} were curve-fitted by the OPUS software (version 6.0) with 10 Gaussian bands, following the recommendation of Li et al. [35]. The assignment of these 10 bands is briefly summarized in Table S2 (Supplementary materials).

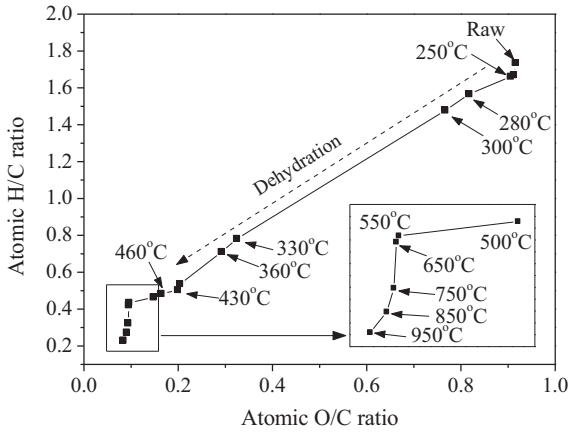

Fig. 2. The Van Krevelan diagram of cellulose char from different temperatures.

The change of crystal structure in cellulose char during pyrolysis was explored with the X-ray diffraction (PANalytical, X'Pert PRO, Netherlands). The maximum power, tube voltage and electric current of the X-ray emitter are 3 KW, 60 KV and 60 mA, respectively. The scanning angle (2θ) ranges from 10° to 90°.

3. Results and discussion

3.1. Chemical composition of cellulose char

The char yield was 75.2% when the temperature was below 300 °C, suggesting that cellulose had been partially pyrolyzed. As the temperature increased, the yield of char decreased remarkably to 18.4% at 430 °C. However, the yield decreased by 14.4% only as the temperature increased from 430 to 950 °C. The result suggested that the depolymerization of cellulose mainly occurred at temperature lower than 430 °C, which was consistent with our previous result that the pyrolysis of cellulose mainly occurred at 315–400 °C [36].

The char was the carbon-rich solid product from pyrolysis, varying from unchanged or barely pyrolyzed cellulose at low temperature to the highly carbonized material at high temperature. Temperature exerts a strong influence on the yield and the chemical composition of the chars (Table S3). An increase of temperature led to a continuous decrease in the yield of char, as a result of either the primary or secondary decomposition of char residue. The carbon content in residual char increased with temperature, whereas that of hydrogen and oxygen decreased gradually.

The Van Krevelan diagram of cellulose char at different temperatures is shown in Fig. 2. It can be seen that the atomic ratios of H/C and O/C decreased gradually when the temperature was below 300 °C, which indicated that dehydration was the predominated reaction. However, a sharp decrease in the H/C value was observed from 1.48 at 300 °C to 0.78 at 330 °C, demonstrating that significant decomposition of cellulose occurred. Meanwhile, the H/C value of 0.78 suggested that a non-condensed aromatic structure or aromatic nucleus with aliphatic side chain was formed in the residual char [37]. Moreover, it showed that dehydration combined with decarbonylation, ring-opening and aromatization seemed to occur when the temperature was above 330 °C.

At 430 °C, the dehydration was almost accomplished and apparently the chemical reactions during pyrolysis changed. As can be seen, the decrease of O/C was more significant than that of H/C in the range of 430–650 °C, suggesting that deoxygenation such as decarbonylation and decarboxylation is predominant over this temperature range. With the further increase in temperature, the value of O/C decreased slightly whereas that of H/C decreased

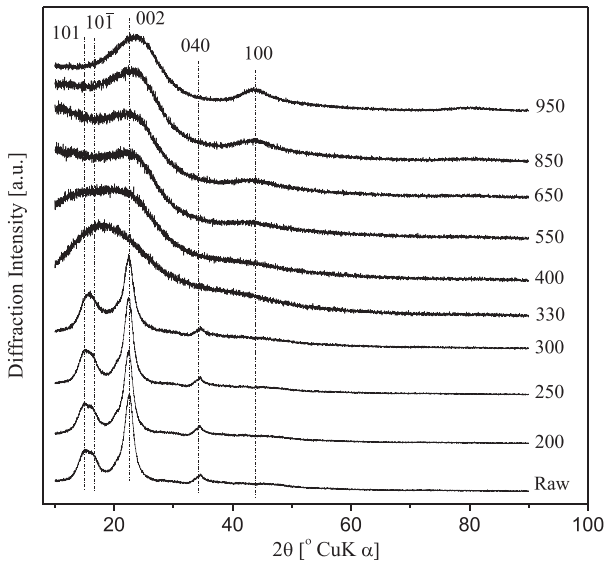

Fig. 3. Typical X-ray diffractograms of cellulose chars.

remarkably from 0.42 at 650 °C to 0.23 at 950 °C. It indicated that the predominated reaction had shifted from deoxygenation toward dehydrogenation, such as demethylation, demethylenation. Furthermore, the atomic ratios of H/C at 950 °C showed that the char was highly aromatic probably due to the condensation of small aromatic ring that formed at lower temperature [37].

3.2. Crystal structure property of cellulose char

Among the biomass constituents, only cellulose is crystalline due to its abundant hydroxyl groups involved in a number of intra- and inter-molecular H-bonds. The X-ray diffractgrams of cellulose char are shown in Fig. 3. The raw cellulose sample displayed typical crystal structure with diffraction peaks for the plane (0 0 2) at $2\theta = 21.2°$, (101) at $2\theta = 14.4°$ and (10$\bar{1}$) at $2\theta = 15.9°$ [10,38]. The diffraction peaks between 14° and 16° merged, while the diffraction peak (0 4 0) was very weak.

As the pyrolysis temperature increased up to 300 °C, it was clear that the residual char was still in the form of crystalline. However, the strong crystalline scatter peaks progressively lost intensity and became broader, indicating a gradual decrease in cellulose crystallinity. Generally, the broadening of band may be due to the decrease in cellulose crystallite thickness, increase in packing defects, or compositional inhomogeneity, etc. [39]. The broadening of band suggested the underlying cleavage of the H-bonds or the scission of glycosidic bonds and pyran ring during the initial pyrolysis stage. Accordingly, it enabled the subsequent aromatization in the residual char at higher temperature. When the temperature was above 300 °C, the crystalline peaks diminished and became invisible at around 400 °C. It suggested that crystal structure of cellulose was lost gradually with the increase of temperature and resulted in the formation of a highly disordered structure in char.

Notably, two broad peaks appeared at 2θ values of around 22.7° and 39.8° for the char obtained above 550 °C. These peaks derived from the diffraction scatter of graphene sheets and planes, suggesting the formation of graphite structure; however, it is obvious that the stacking of graphene sheets is substantially disordered. With temperature increasing further, the narrowing of these peaks indicated a progressive stacking of graphene sheets and the lateral growth of graphene planes, which resulted in the formation of crystallites [40].

3.3. Surface functionality transformation of cellulose char at low temperature

The IR spectrum is complex and has been generally separated into two regions: the —OH and —CH vibrations in the range of 3800–2700 cm^{-1} and the "fingerprint" region located at 1800–800 cm^{-1}. Band assignments of a typical IR spectrum of cellulose are summarized in Table 1. It is noted that the —OH stretching models comprise different hydrogen bonding forms in the range of 3800–3000 cm^{-1}.

Fig. S1 shows the infrared spectrum of raw cellulose and the resultant chars (Supplementary material). It was evident that cellulose char still remained a crystal form at temperature lower than 330 °C, which is consistent with the X-ray diffraction analysis results. However, the absorbance intensity of the bands in 900–1500 cm^{-1} region corresponding to glycosidic bond and glucose unit decreased gradually as the temperature increased. The intensities of these bands as well as the hydroxyl group all decreased at 330 °C, indicating the drastic decomposition of cellulose. Meanwhile, the intensity of the bands in 1500–1800 cm^{-1} region increased remarkably. With the further increase of temperature, the intensities of glycosidic bond, glucose unit and hydroxyl groups decreased continuously and almost vanished when the temperature exceed 500 °C. It means that the residual char was free of organic functional groups at this temperature range.

In order to clarify the overlapped information in conventional infrared spectra, the spectra were analyzed with 2D correlation spectroscopy method. The synchronous and asynchronous 2D correlation spectrum of cellulose char in the region of 3700–2700 cm^{-1} was plotted in Fig. 4. There was a strong auto peak at around 3350 cm^{-1} and a weaker one at 2900 cm^{-1}, which indicate that the O(3)H···O(5) intra-molecular H-bonds were the most sensitive to temperature. This is consistent with the results from Watanabe who found that the O(3)H3···O(5) intrachain H-bonds in cellulose changed at temperature as low as 25 °C and progressively greater above 130 °C [30]. Furthermore, compared to —CH of pyran ring and other hydrogen bonds, the hydrogen bonds changed to a greater degree in response to the increase of pyrolysis temperature. A positive cross peak Φ(3350,2900) located at the off-diagonal position of synchronous spectrum suggested that O(3)H···O(5) intra-molecular hydrogen bond and the —CH of pyran ring changed coincidentally with the increase of pyrolysis temperature. In addition, the absorption band corresponding to the olefins at 3014 cm^{-1} formed two negative cross peaks with 3350 cm^{-1} and 2900 cm^{-1}. It suggested that the change of olefin was negatively related to that of H-bonds and —CH.

In the asynchronous 2D correlation spectrum, five bands at 3500 cm^{-1}, 3230 cm^{-1}, 3018 cm^{-1}, 2928 cm^{-1}, and 2877 cm^{-1} were observed and formed positive cross peaks with 3350 cm^{-1} and 2900 cm^{-1} in the asynchronous spectra, such as Ψ(3500, 3350), Ψ(3230, 3350), etc. According to Noda's rules [27], the sequences of spectral change can be derived as follows: (3500,3230,2877) > 3350 > 2928 > 3014. It indicated that the change of O(3)H···O(5) intra-molecular H-bond occurred after that of O(2)H···O(6) intra-molecular, O(6)H···O(3) inter-molecular H-bond and glucopyranose ring —CH, but occurred predominantly before that of the methylene and olefin groups. This was in line with the fact that the energy of O(2)H...O(6) intra-molecular H-bond is the weakest among the H-bonds in cellulose structure [25]. Agarwal et al. also found that O(2)H...O(6) intrachain H-bonds tend to be convertedto other interchain hydrogen bonds [32]. Furthermore, the cleavage of O(6)H···O(3) H-bond was likely to occur coincidentally with O(2)H···O(6) H-bonds. Since the hydroxyl groups at C6 position were more likely to form inter-molecular H-bonds rather than intra-molecular H-bonds, the cleavage of inter-molecular H-bonds and dehydration will presumably result in the formation of

Table 1
The main functional groups of cellulose.

Wavenumber (cm^{-1})	Infrared absorption	Functional groups and structures
3500	OH stretching	O(2)H···O(6) intramolecular hydrogen bonds
3350	OH stretching	O(3)H···O(5) intramolecular hydrogen bonds
3230	OH stretching	O(6)H···O(3) intermolecular hydrogen bonds
3018	CH stretching	Aromatic structure
2928	CH stretching	C6-methylene of glucopyranose ring
2900, 2877	CH stretching	—CH of glucopyranose ring
1714	C=O stretching	Saturated ketone carbonyl
1705	C=O stretching	Non-conjugated carbonyl
1610	C=C stretching	Olefins conjugated with aromatic ring
1603	C=C stretching	Olefins Conjugated with double bonds or carbonyl
1585	C=C stretching	Aromatic structure
1252	C—O stretching	Cyclic ethers, Aryl alkyl ether
1163	C—O stretching	Glycosidic bond
1146	C—O stretching	Aliphatic ether
1113	C—O stretching	Glucose pyran ring
1060	C—O stretching	Hydroxyl group

olefins [29]. Generally, the thermally induced cleavage of H-bonds in cellulose will firstly lead to the formation of free hydroxyl groups. Nevertheless, free hydroxyl were not observed in this study, suggesting that it underwent subsequent dehydration and resulted in the formation of water as well as double-bonded olefin in bio-char.

The relative intensities of different absorption peaks at 3700–2700 cm^{-1} for char resulted from cellulose pyrolysis are shown in Fig. 5. As can be seen from Fig. 5(a), the decrease in the intensity of —OH vibration demonstrated that dehydration could occur at temperature as low as 200 °C. Although most of the previous works regarded that no chemical elimination of water occurred from crystal cellulose before 220 °C [41], the result in this study indicated that the chemical evolution of water could take place even at 200 °C. Pastorova et al. [42] pyrolyzed cellulose at 190 °C and 220 °C for 2.5 h under nitrogen and observed 8% and 10% weight loss of cellulose, respectively. However, the weight loss is about 1% in the present study, probably due to the shorter heating duration of solid. This suggested that the heating durations might be an influential factor for low temperature pyrolysis. With the increase of residence time, the evolved water might in turn serve as catalyst to accelerate the depolymerization and dehydration [41]. The above results suggested that 200 °C was likely to be the initial temperature at which water can be evolved from cellulose chemically. Furthermore, the intensity of intra-molecular H-bonds was lower than that of inter-molecular H-bonds as temperature lower than 300 °C. This is in agreement with the results from previous study that O(3)H3···O(5) and O(2)H2···O(6) intrachain H-bonds mainly occurred in 30–200 °C [31].

The intra- and inter-molecular H-bonds and pyran ring —CH showed a remarkable decrease in relative intensity as the pyrolysis temperature increased up to 300 °C. Furthermore, the intensity of intra-molecular H-bonds was apparently lower than that of inter-molecular H-bonds, probably because hydroxyl groups at C2 and C3 position were more active than that at C6 position [8]. The cellulose pyrolysis led to a weight loss of about 25% at 300 °C, and XRD results suggested that the residual char was still crystalline. It suggested that dehydration was the predominated reactions during the initial stage of pyrolysis and mostly among the intra-molecular H-bonds. Moreover, dehydration in this stage probably resulted in the decrease in the crystallinity of char (Fig. 3).

When the temperature was above 300 °C, the intensities of inter-molecular H-bonds as well as methylene groups decreased significantly, suggesting the disassociation of cellulose chain among the microfibers. As a result, the crystallinity and linearity of cellulose disappeared. It was likely to configurate a three-dimensional network polymer at 300 °C [24]. Meanwhile, Fig. 5(b) clearly shows that the intensity of olefins increased remarkably, indicating that dehydration had been accelerated. The —OH and —CH vibrations exhibited a low intensity at about 430 °C, indicating that dehydration was almost accomplished.

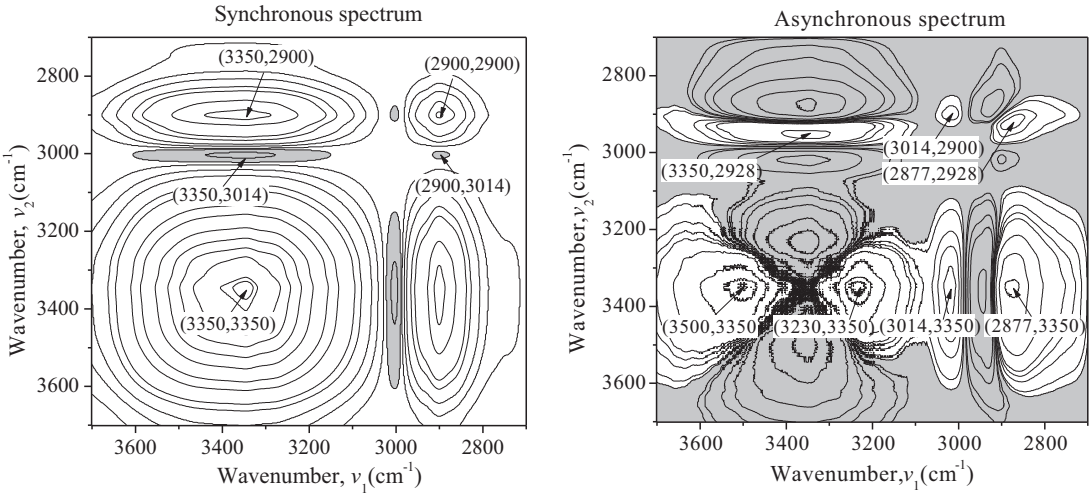

Fig. 4. Synchronous and asynchronous 2D correlation spectra in the OH-stretch and CH-stretch (3700–2700 cm^{-1}) constructed from the temperature-dependent IR spectra of chars produced under nitrogen for 30 min, and pyrolysis temperature between 200 and 650 °C. Light gray and white areas indicate negative and positive correlation values, respectively.

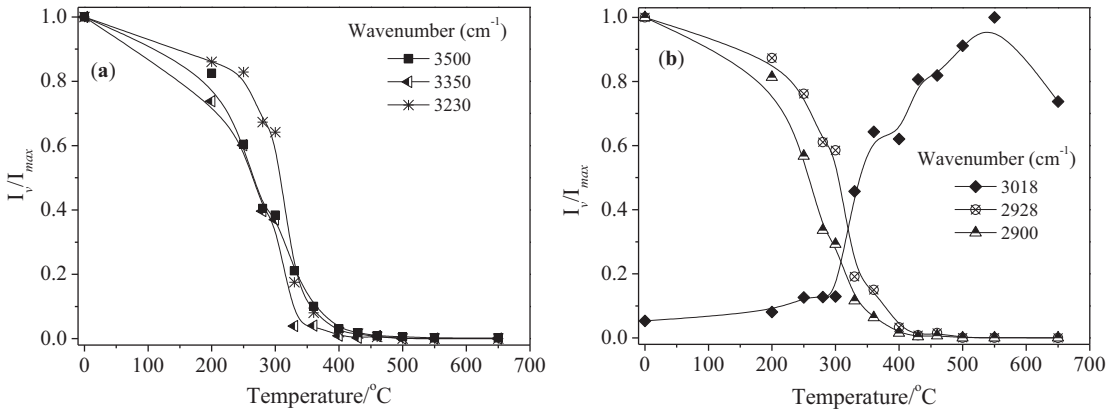

Fig. 5. Variation in the relative intensities (I_v/I_{max}: for a given peak intensity/the maximum peak intensity) of peaks in synchronous and asynchronous 2D correlation spectra (3700–2700 cm^{-1}) for the chars produced under nitrogen for 30 min, and pyrolysis temperature between 200 and 650 °C.

The synchronous and asynchronous 2D correlation spectra in the "fingerprint" region are presented in Fig. 6. In synchronous spectrum, five main auto peaks were identified. The auto peaks observed in the region of 1800–1600 cm^{-1} and 1200–1000 cm^{-1} formed positive cross peaks with each other, such as Φ(1705,1603), Φ(1163,1113), etc, suggesting that carbonyl and conjugated olefin changed coincidentally with the pyrolysis temperature. Similar trends were also observed in glycosidic bond, glucose pyran ring and the hydroxyl group during pyrolysis. Meanwhile, positive cross peaks at Φ(1705,1252) and Φ(1603,1252) demonstrated that the change of ether groups during pyrolysis was similar with carbonyl and conjugated olefin. The negative cross peaks Φ(1705,1163) and Φ(1603,1163) indicated that the changing trend of carbonyl and conjugated olefin groups is opposite to that of glycosidic bond and glucose pyran ring. Since the latter are the inherent groups of unaltered cellulose, it was speculated that carbonyl, olefins and ethers were formed at the expense of these characteristic groups.

In asynchronous 2D correlation spectrum, the absorption peak was observed at 1610 cm^{-1} corresponding to the olefin conjugated with aromatic ring or double bonds [43,44]. Similar observations were also made for the band at 1714 cm^{-1}, which was characteristic of saturated aliphatic carbonyl [45]. This suggested that the evolution in the structure of substitution groups which were grafted on the olefin double bonds or carbonyl structures had occurred during pyrolysis. The peaks at 1705 cm^{-1} and 1610 cm^{-1} formed a series of positive cross peaks with 1163 cm^{-1}, 1113 cm^{-1} and 1060 cm^{-1}. According to Noda rules, carbonyl and conjugated olefin predominantly occurred before that of glycosidic bond and glucose pyran ring. Therefore, it can be concluded that the cleavage of intramolecular dehydration among hydroxyls at C2 and C3 position will lead to the formation of carbonyl and double-bonded structure in char. In addition, the conjugated olefins were probably in the form of cycloolefins or conjugated with aromatics. Tang and Bacon [20] believed that the carbonyl and double-bonds formed in char essentially resulted from intra-molecular dehydration rather than inter-molecular dehydration. The band at 1163 cm^{-1}, 1113 cm^{-1}, and 1060 cm^{-1} formed three positive cross peaks with the band at 1252 cm^{-1}, suggesting that glycosidic bond and glucose pyran ring occurred predominantly before that of ethers. Moreover, these ethers are mainly composed of cyclic and aromatic ether. The presence of aliphatic ether at 1146 cm^{-1} formed a positive cross peak with the pyran ring at 1113 cm^{-1}, suggesting that the opening of pyran ring occurred before that of aliphatic ether.

The relative intensity of different absorption peaks between 1800 cm^{-1} and 900 cm^{-1} was shown in Fig. 7. It was clear that the intensity of carbonyl and conjugated olefin was very low when the temperature was below 300 °C whereas the intensity of ethers was much higher. The result was likely due to the decomposition of amorphous portion within microcrystalline cellulose [7,46]. The dehydration among hydroxyls on pyran ring or degraded glucan

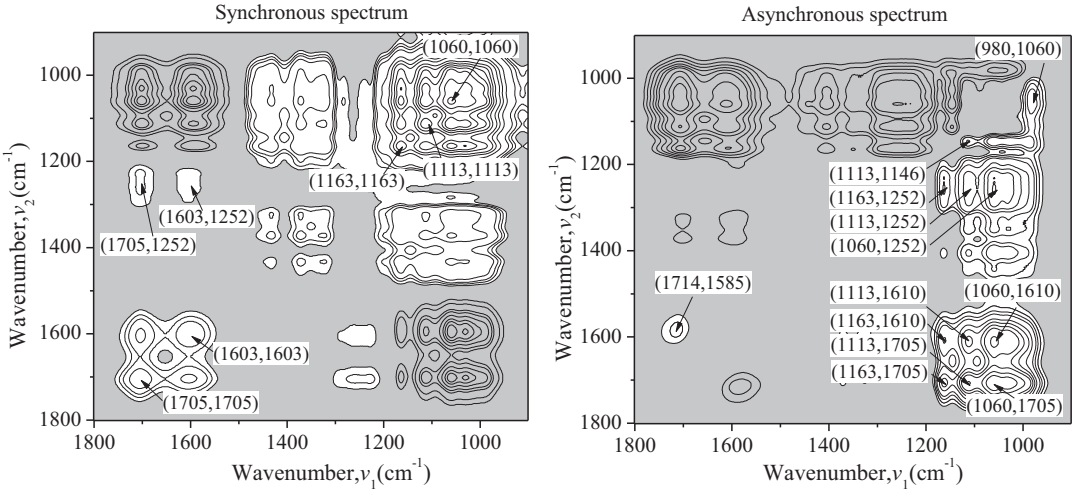

Fig. 6. Synchronous and asynchronous 2D correlation spectra in the 1800–900 cm^{-1} region from chars produced under nitrogen for 30 min, and pyrolysis temperature between 200 and 650 °C. Light gray and white areas indicate negative and positive correlation values, respectively.

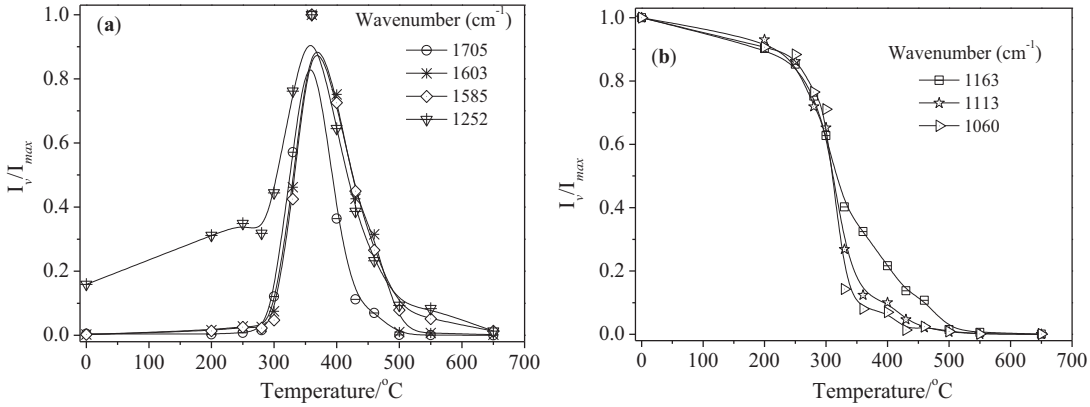

Fig. 7. Variation in the relative intensities of peaks in synchronous and asynchronous 2D correlation spectra (1800-900 cm^{-1}) for the chars produced under nitrogen for 30 min, and pyrolysis temperature between 200 and 650 °C.

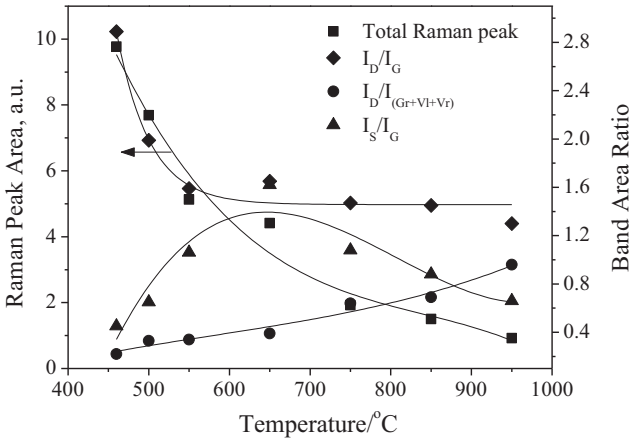

Fig. 8. Changes in the total Raman peak area and the band ratios in the region 1800–800 cm^{-1} as a function of pyrolysis temperature.

chains may result in the formation of cyclic ethers. Moreover, the loss of amorphous cellulose and degradation was mainly responsible for the decrease in the intensities of glycosidic bond and pyran ring as shown in Fig. 7(b).

As the temperature exceeded 300 °C, the intensity of glycosidic bond and pyran ring decreased remarkably. On the contrary, the intensities of carbonyl, conjugated olefin, ether and aromatic structure showed a sharp increase and reached the maximum at 360 °C. The cleavage of glycosidic bond and the breakdown of pyran ring resulted in the formation of aliphatic hydrocarbons which were rich in double bonds, carbonyl and paraffinic branches. As a result, abundant anhydro-saccharides and low oxygenates were identified in liquid bio-oil in our previous study [6]. In addition, the aromatization of aliphatic hydrocarbons can also occur at 300–360 °C, which is consistent with previous results in this study (Fig. 2). With the increase in the concentration of aromatics in char, the solid char appeared to generate alkyl-aryl structures or aromatic ethers during pyrolysis. Sekiguchi et al. [22] found that the majority of aromatics in the cellulose char obtained at 300–400 °C was in the form of phenol and the aromatics were linked with aliphatic hydrocarbons through the C—O bonds. Therefore, it can be concluded that the oligosaccharides, aliphatic hydrocarbons and aromatics formed a disordered three-dimensional bonding network. Agarwal et al. also found such a three-dimensional network during cellulose pyrolysis. However, the author regarded that the network was formed due to the formation of new interchain hydrogen bonds [32]. The changes in the intensity of glycosidic bond and pyran ring seemed to provide further evidence to support the above conclusions. It can be observed from Fig. 7(b)that the decrease in the intensity of glycosidic bond was slower than that of pyran ring. However, the quantum calculation indicated that the bond energy of C—O in glycosidic bond was lower than that of pyran ring [47]. The possible explanation was that parts of the oligosaccharides were bonded together with ether and thus certain amount of glycosidic bond was preserved in the char.

With the temperature increasing further, the intensities of carbonyl, conjugated olefin, ether and aromatic ring decreased rapidly, which suggested that char particles underwent dehydrogenation, decarbonylation, aromatization and condensation as the temperature exceeded 360 °C. The results indicated that the char obtained at 360–550 °C was dehydrated, disordered, carbonized and aromatized. Furthermore, the degree of aromatization was enhanced with pyrolysis temperature increasing.

3.4. Structure evolution of cellulose char at higher temperature

Fig. 8 shows the total Raman peak areas and band ratios between 1800 and 800 cm^{-1} as a function of temperature. Fig. S2 presents a visible comparison between Raman spectrum of different chars that was obtained following the aforementioned procedures and the curve-fitted Raman spectrum of cellulose char obtained at 750 °C (Supplementary material). It can be seen that total Raman peak area decreased constantly with the increase of pyrolysis temperature. Generally, the aromatization of char during pyrolysis resulted in the increases of the light absorbing ability and thus decreasing Raman intensity [48]. Furthermore, the decrease in Raman intensity was also attributed to the loss of O-containing structures in the residual char since the electron-rich functional groups such as those containing oxygen appear high in Raman intensity [35]. In biomass char, the ratio of I_D/I_G is widely used to measure the crystalline or graphite-like carbon structures and the decrease in this ratio is usually expected with the increase of the degree of graphitization [49]. However, the biomass chars formed at low temperature was a disorder polymer and the size of aromatic rings in the char was far from the size required for generating graphite crystals [35,40]. Hence, the decrease in the ratio of I_D/I_G in this study indicated the development of aromatic ring systems in char, particularly the smaller aromatic systems. It was noted that the decrease of the ratio of I_D/I_G in the range of 450–650 °C was larger than that observed at high temperatures (750–950 °C). According to the chemical analysis, deoxygenation was the predominant reactions that occurred in this temperature range. Therefore, it was reasonable to speculate that deoxygenation and condensation occurred in the individual

benzene ring or smallest aromatic clusters grafted with oxygenated groups in char, and the resultant char contained large portions of smaller aromatic systems, i.e., 2–6 fused ring structures. It also demonstrated that the concentration of larger aromatic rings with more than six rings was very low in the char obtained at lower temperature.

As the temperature exceeded 650 °C, the ratio of I_D/I_G remained relatively stable whereas the ratio of $I_D/I_{(Gr+Vl+Vr)}$ increased gradually with the increase of temperature. Generally, the ratio of $I_D/I_{(Gr+Vl+Vr)}$ is widely used to measure the relative proportions between large (≥6 rings) aromatic ring systems and small systems found in amorphous carbon [35]. Therefore, this observation indicated the enlargement of aromatic ring systems in the residual char. Moreover, the changes in this ratio at lower temperature range (450–650 °C) was much smaller than that at higher temperature range (650–950 °C), suggesting that the dehydrogenation of hydroaromatics and the condensation among small aromatics have been accelerated during pyrolysis in the high temperature range. This is consistent with the result of the elemental analysis of char for which dehydrogenation was the predominant reaction that occurred in the range of 650–950 °C.

The S band in biomass chars mainly represents the alkyl-aryl structures, aromatic (aliphatic) ethers, and methyl carbon grafted to an aromatic ring and thus can be used as the measurement of cross-linking density and substitution groups in char [49]. As shown in Fig. 8, the ratio I_S/I_G increased remarkably from 450 to 650 °C, suggesting the increase in the level of cross-linked network structure in the residual char, which resulted from the crosslinking reactions during pyrolysis. Moreover, the crosslinking reactions were likely to occur after decarboxylation or loss of O-containing functional groups [35]. The ratio of I_S/I_G decreased progressively as the temperature increased further, suggesting the loss of alkyl and ether structure as a result of dehydrogenation, demethylation or condensation among small aromatics. Therefore, the cross-linked density of char decreased and the char obtained at higher temperatures tended to form highly ordered graphitic structure. Nevertheless, the char produced at temperature as high as 950 °C still contains certain amount of alkyl-aryl and ether structure and this indicated that new alkyl-aryl structures form continuously during pyrolysis.

4. Conclusions

The formation of chemical structure of char during cellulose (ash-free) pyrolysis at various temperatures was investigated in depth. It was found that 200 °C is likely to be the initial temperature at which water can be evolved chemically. When the temperature is lower than 300 °C, cellulose underwent the cleavage of intra- and inter-molecular H-bonds. Meanwhile, the subsequent dehydration was the predominant reaction that mainly occurred among the intra-molecular H-bonds. The O(2)H···O(6) intra-molecular, O(6)H···O(3) inter-molecular H-bonds and pyran ring —CH cleaved first, followed by the cleavage of O(3)H···O(5) intra-molecular H-bonds. Then, the concentration of methylene decreased and olefin began to form. When the temperature was over 300 °C, the concentration of carbonyl, conjugated olefin, ether and aromatic structure increased greatly in the expense of glycosidic bond, pyran ring and hydroxyl groups that diminished in the residual char. Furthermore, the oligosaccharides, aliphatic hydrocarbons and aromatics formed a disordered three-dimensional bonding network through the ether linkage.

At 430–650 °C, the smallest aromatic clusters grafted with oxygenated groups underwent significant deoxygenation and condensation. The aromatic ring systems increased in amount and size with the further increase of temperature. When the temperature was higher than 650 °C, the predominated reaction shifted from deoxygenation to dehydrogenation. Meanwhile, the char was highly aromatic with more than six aromatic rings fused together. The result of this study can help understand the initial stage chemistry and carbon structure evolution during cellulose pyrolysis.

Acknowledgments

The authors wish to express the great appreciation of the financial support from National Basic Research Program of China (973 Program) (2013CB228102), and National Natural Science Foundation of China (51376076 and 51306066) and the Special Fund for Agro-scientific Research in the Public Interest (201303095). The experiment was also assisted by Analytical and Testing Center in Huazhong University of Science & Technology (http://atc.hust.edu.cn), Wuhan 430074 China. Mr. Ho Simon Wang has helped improve the linguistic presentation of the manuscript.

Appendix A. Supplementary data

Supplementary data associated with this article can be found, in the online version, at http://dx.doi.org/10.1016/j.jaap.2015.09.002.

References

[1] A. Demirbas, G. Arin, An overview of biomass pyrolysis, Energy Sources 24 (2002) 471–482.
[2] M. Peter, Energy production from biomass (part 1): overview of biomass, Bioresour. Technol. 83 (2002) 37–46.
[3] R.C. Sun, Cereal Straw as a Resource for Sustainable Biomaterials and Biofuels: Chemistry, Extractives, Lignins, Hemicelluloses and Cellulose, Elsevier Science, 2010.
[4] K.H. Gardner, J. Blackwell, The structure of native cellulose, Biopolymers 13 (1974) 1975–2001.
[5] K.H. Gardner, J. Blackwell, The hydrogen bonding in native cellulose, Biochim. Biophys. Acta (BBA)—Gen. Subj. 343 (1974) 232–237.
[6] S. Xin, H. Yang, Y. Chen, X. Wang, H. Chen, Assessment of pyrolysis polygeneration of biomass based on major components: product characterization and elucidation of degradation pathways, Fuel 113 (2013) 266–273.
[7] D. Liu, Y. Yu, H. Wu, Differences in water-soluble intermediates from slow pyrolysis of amorphous and crystalline cellulose, Energy Fuels 27 (2013) 1371–1380.
[8] M. Zhang, Z. Geng, Y. Yu, Density functional theory (DFT) study on the dehydration of cellulose, Energy Fuels 25 (2011) 2664–2670.
[9] P.R. Patwardhan, D.L. Dalluge, B.H. Shanks, R.C. Brown, Distinguishing primary and secondary reactions of cellulose pyrolysis, Bioresour. Technol. 102 (2011) 5265–5269.
[10] J. Zhang, J. Luo, D. Tong, L. Zhu, L. Dong, C. Hu, The dependence of pyrolysis behavior on the crystal state of cellulose, Carbohydr. Polym. 79 (2010) 164–169.
[11] Q. Lu, X.C. Yang, C.Q. Dong, Z.F. Zhang, X.M. Zhang, X.F. Zhu, Influence of pyrolysis temperature and time on the cellulose fast pyrolysis products: analytical Py-GC/MS study, J. Anal. Appl. Pyrolysis 92 (2011) 430–438.
[12] R. Lanza, D. Dalle Nogare, P. Canu, Gas phase chemistry in cellulose fast pyrolysis, Ind. Eng. Chem. Res. 48 (2009) 1391–1399.
[13] S. Li, J. Lyons-Hart, J. Banyasz, K. Shafer, Real-time evolved gas analysis by FTIR method: an experimental study of cellulose pyrolysis, Fuel 80 (2001) 1809–1817.
[14] J.B. Wooten, J.I. Seeman, M.R. Hajaligol, Observation and characterization of cellulose pyrolysis intermediates by 13C CPMAS NMR. A new mechanistic model, Energy Fuels 18 (2003) 1–15.
[15] A. Demirbas, Effects of temperature and particle size on bio-char yield from pyrolysis of agricultural residues, J. Anal. Appl. Pyrolysis 72 (2004) 243–248.
[16] P. Fu, S. Hu, L. Sun, J. Xiang, T. Yang, A. Zhang, J. Zhang, Structural evolution of maize stalk/char particles during pyrolysis, Bioresour. Technol. 100 (2009) 4877–4883.
[17] R.K. Sharma, M.R. Hajaligol, Effect of pyrolysis conditions on the formation of polycyclic aromatic hydrocarbons (PAHs) from polyphenolic compounds, J. Anal. Appl. Pyrolysis 66 (2003) 123–144.
[18] A.G.W. Bradbury, Y. Sakai, F. Shafizadeh, A kinetic model for pyrolysis of cellulose, J. Appl. Polym. Sci. 23 (1979) 3271–3280.
[19] S. Matsuoka, H. Kawamoto, S. Saka, What is active cellulose in pyrolysis? an approach based on reactivity of cellulose reducing end, J. Anal. Appl. Pyrolysis 106 (2014) 138–146.
[20] M.M. Tang, R. Bacon, Carbonization of cellulose fibers—I. low temperature pyrolysis, Carbon 2 (1964) 211–220.

[21] F. Shafizadeh, Y. Sekiguchi, Development of aromaticity in cellulosic chars, Carbon 21 (1983) 511–516.
[22] Y. Sekiguchi, J.S. Frye, F. Shafizadeh, Structure and formation of cellulosic chars, J. Appl. Polym. Sci. 28 (1983) 3513–3525.
[23] J.J. Boon, I. Pastorova, R. Botto, P. Arisz, Structural studies on cellulose pyrolysis and cellulose chars by PYMS, PYGCMS, FTIR, NMR and by wet chemical techniques, Biomass Bioenergy 7 (1994) 25–32.
[24] I. Pastorova, R.E. Botto, P.W. Arisz, J.J. Boon, Cellulose char structure: a combined analytical Py-GC–MS, FTIR, and NMR study, Carbohydr. Res. 262 (1994) 27–47.
[25] C.-M. Popescu, M.-C. Popescu, C. Vasile, Structural analysis of photodegraded lime wood by means of FT-IR and 2D IR correlation spectroscopy, Int. J. Biol. Macromol. 48 (2011) 667–675.
[26] M.-C. Popescu, J. Froidevaux, P. Navi, C.-M. Popescu, Structural modifications of Tilia cordata wood during heat treatment investigated by FT-IR and 2D IR correlation spectroscopy, J. Mol. Struct. 1033 (2013) 176–186.
[27] I. Noda, Y. Ozaki, Two-Dimensional Correlation Spectroscopy: Applications in Vibrational and Optical Spectroscopy, John Wiley & Sons, New York, 2004.
[28] I. Noda, A. Dowrey, C. Marcott, G. Story, Y. Ozaki, Generalized two-dimensional correlation spectroscopy, Appl. Spectrosc. 54 (2000) 236A–248A.
[29] O.R. Harvey, B.E. Herbert, L.J. Kuo, P. Louchouarn, Generalized two-dimensional perturbation correlation infrared spectroscopy reveals mechanisms for the development of surface charge and recalcitrance in plant-derived biochars, Environ. Sci. Technol. 46 (2012) 10641–10650.
[30] A. Watanabe, S. Morita, Y. Ozaki, Temperature-dependent structural changes in hydrogen bonds in microcrystalline cellulose studied by infrared and near-infrared spectroscopy with perturbation-correlation moving-window two-dimensional correlation analysis, Appl. Spectrosc. 60 (2006) 611–618.
[31] A. Watanabe, S. Morita, Y. Ozaki, Study on temperature-dependent changes in hydrogen bonds in cvellulose Iβ by infrared spectroscopy with perturbation-correlation moving-window two-dimensional correlation spectroscopy, Biomacromolecules 7 (2006) 3164–3170.
[32] V. Agarwal, G.W. Huber, W.C. Conner, S.M. Auerbach, Simulating infrared spectra and hydrogen bonding in cellulose Iβ at elevated temperatures, J. Chem. Phys. 135 (2011) 134506.
[33] D. Shen, R. Xiao, S. Gu, K. Luo, The pyrolytic behavior of cellulose in lignocellulosic biomass: a review, RSC Adv. 1 (2011) 1641–1660.
[34] Y. Chen, B. Liu, H. Yang, Q. Yang, H. Chen, Evolution of functional groups and pore structure during cotton and corn stalks torrefaction and its correlation with hydrophobicity, Fuel 137 (2014) 41–49.
[35] X. Li, J. -i. Hayashi, C.-Z. Li, FT-Raman spectroscopic study of the evolution of char structure during the pyrolysis of a Victorian brown coal, Fuel 85 (2006) 1700–1707.
[36] H. Yang, R. Yan, H. Chen, D.H. Lee, C. Zheng, Characteristics of hemicellulose, cellulose and lignin pyrolysis, Fuel 86 (2007) 1781–1788.
[37] S.A. Visser, Application of Van Krevelen's graphical-statistical method for the study of aquatic humic material, Environ. Sci. Technol. 17 (1983) 412–417.
[38] R. Liu, H. Yu, Y. Huang, Structure and morphology of cellulose in wheat straw, Cellulose 12 (2005) 25–34.
[39] M.-C. Popescu, C.-M. Popescu, G. Lisa, Y. Sakata, Evaluation of morphological and chemical aspects of different wood species by spectroscopy and thermal methods, J. Mol. Struct. 988 (2011) 65–72.
[40] M. Keiluweit, P.S. Nico, M.G. Johnson, M. Kleber, Dynamic molecular structure of plant biomass-derived black carbon (Biochar), Environ. Sci. Technol. 44 (2010) 1247–1253.
[41] J. Scheirs, G. Camino, W. Tumiatti, Overview of water evolution during the thermal degradation of cellulose, Eur. Polym. J. 37 (2001) 933–942.
[42] I. Pastorova, P.W. Arisz, J.J. Boon, Preservation of D-glucose-oligosaccharides in cellulose chars, Carbohydr. Res. 248 (1993) 151–165.
[43] Y. Ke, H. Dong, Handbook of Analytical Chemistry—Spectroscopy, vol. 3, Chemical Industry Press, Beijing, 1998.
[44] R.R.M. Silverstein, F.X. Webster, D.J. Kiemle, The Spectrometric Identification of Organic Compounds, John Wiley & Sons, New York, 2005.
[45] S. Weng, Fourier Transform Infrared Spectroscopy, Chemical Industry Press, Beijing, 2010.
[46] Y. Yu, D. Liu, H. Wu, Characterization of water-soluble intermediates from slow pyrolysis of cellulose at low temperatures, Energy Fuels 26 (2012) 7331–7339.
[47] J. Huang, Molecular Simulation Study of Pyrolysis Mechanism of Cellulose, Chongqing University, College of Power Engineering, 2010, 2015.
[48] M. Asadullah, S. Zhang, C.-Z. Li, Evaluation of structural features of chars from pyrolysis of biomass of different particle sizes, Fuel Process. Technol. 91 (2010) 877–881.
[49] D.M. Keown, X. Li, J. -i. Hayashi, C.-Z. Li, Characterization of the structural features of char from the pyrolysis of cane trash using fourier transform-Raman spectroscopy, Energy Fuels 21 (2007) 1816–1821.